IEEE Access
Multidisciplinary | Rapid Review | Open Access Journal

Received February 3, 2019, accepted March 2, 2019, date of publication March 5, 2019, date of current version March 26, 2019.

Digital Object Identifier 10.1109/ACCESS.2019.2903210

Congestion Management Method of Low-Voltage Active Distribution Networks Based on Distribution Locational Marginal Price

JINLI ZHAO[1], (Member, IEEE), YUSHUO WANG[1], GUANYU SONG[1], (Member, IEEE), PENG LI[1], (Member, IEEE), CHENGSHAN WANG[1], (Senior Member, IEEE), AND JIANZHONG WU[2], (Member, IEEE)

[1]Key Laboratory of Smart Grid of Ministry of Education, Tianjin University, Tianjin 300072, China
[2]School of Engineering, Institute of Energy, Cardiff University, Cardiff CF24 3AA, U.K.

Corresponding author: Guanyu Song (gysong@tju.edu.cn)

This work was supported by the National Natural Science Foundation of China under Grant U1866207 and Grant 51807132.

ABSTRACT Large-scale distributed energy resources, such as electric vehicles (EVs) asymmetric access to low-voltage distribution systems, may cause security problems, including line congestion, voltage violation, and three-phase unbalance. In this paper, a congestion management method of low-voltage active distribution networks is proposed. The soft open point, a flexible power electronic device, is considered as a direct control means to solve the congestion problem first. A semidefinite programming model based on a symmetrical component method is constructed to optimize the operation strategy that can be efficiently solved to meet the demands of rapid centralized control. To guide the charging behaviors of flexible load represented by EVs, a market mechanism suitable for the low-voltage unbalanced network is further considered. Though linear approximation and sensitivity analysis, a pricing model of flexible load is established accounting for the effect of network loss, voltage variation, voltage three-phase unbalance, and line overload to distribution locational marginal price. Case studies are carried out on the modified IEEE 33-node and IEEE 123-node system to verify the effectiveness and efficiency of the proposed method.

INDEX TERMS Congestion management, unbalance, distribution locational marginal price (DLMP), soft open point (SOP), semidefinite programming (SDP), sensitivity analysis.

NOMENCLATURE

Sets

Ω_b	Set of all branches
$\mathcal{N}$	Set of nodes that are not root nodes
Φ_i	Set of phases for node i, $\Phi_i \subseteq \{a, b, c\}$
Φ_{ij}	Set of phases for branch ij, $\Phi_{ij} \subseteq \{a, b, c\}$

Indices

i, j	Indices of nodes
φ	Indices of phases, referring to a, b and c
l	Indices of branches

Variables

$V_{\varphi,i}$, V_i	Complex voltage on phase φ of node i defined as $V_i := (V_{\varphi,i}, \varphi \in \Phi_i) \in C^{\lvert\Phi_i\rvert}$
$I_{\varphi,ij}$, I_{ij}	Complex current on phase φ of branch ij, defined as $I_{ij} := (I_{\varphi,ij}, \varphi \in \Phi_{ij}) \in C^{\lvert\Phi_{ij}\rvert}$
$s_{\varphi,i}$, s_i	Complex power injection on phase φ of node i, defined as $s_i := (s_{\varphi,i}, \varphi \in \Phi_i) \in C^{\lvert\Phi_i\rvert}$
v_i, l_{ij}	Auxiliary variables that indicate $v_i := V_i V_i^{\mathrm{H}} \in H^{\lvert\Phi_i\rvert\times\lvert\Phi_i\rvert}$, and $l_{ij} := I_{ij} I_{ij}^{\mathrm{H}} \in H^{\lvert\Phi_{ij}\rvert\times\lvert\Phi_{ij}\rvert}$
v_i^{012}, l_{ij}^{012}	Auxiliary variables in symmetrical components that indicate $v_i^{012} := A^{\mathrm{H}} V_i V_i^{\mathrm{H}} A \in H^{\lvert\Phi_i\rvert\times\lvert\Phi_i\rvert}$, and $l_{ij}^{012} := A^{\mathrm{H}} I_{ij} I_{ij}^{\mathrm{H}} A \in H^{\lvert\Phi_{ij}\rvert\times\lvert\Phi_{ij}\rvert}$
S_{ij}	Complex power flow of branch ij, defined as $S_{ij} = V_i I_{ij}^{\mathrm{H}} \in C^{\lvert\Phi_{ij}\rvert\times\lvert\Phi_{ij}\rvert}$
S_{ij}^{012}	Complex power flow of branch ij in symmetrical components defined as $S_{ij}^{012} = A^{\mathrm{H}} V_i I_{ij}^{\mathrm{H}} A \in C^{\lvert\Phi_{ij}\rvert\times\lvert\Phi_{ij}\rvert}$
$P_{\varphi,i,t}^{\mathrm{EV}}$	Active power injection by EV on phase φ of node i at period t

The associate editor coordinating the review of this manuscript and approving it for publication was Salvatore Favuzza.

$P_{\varphi,i,t}^{\mathrm{EV,flx}}$	Flexible charging power by EV on phase φ of node i at period t
$P_{\varphi,i}^{\mathrm{DG}}$, $Q_{\varphi,i}^{\mathrm{DG}}$	Active/reactive power injection by DG on phase φ of node i
$\tan\theta_{\varphi,i}^{\mathrm{DG}}$	$\cos\theta_{\varphi,i}^{\mathrm{DG}}$ is the power factor of DG on phase φ of node i
$P_{\varphi,i}^{\mathrm{SOP}}$, $Q_{\varphi,i}^{\mathrm{SOP}}$	Active/reactive power injection by SOP on phase φ of node i
$P_i^{\mathrm{SOP,loss}}$	Active power losses of the SOP of node i
Parameters	
σ_t^{r}	Electricity purchase price of active power of DSO at period t
σ_t^{EV}	Bidding price of active power of EV at period t
$\alpha_{\varphi,i}$	Proportion of EV with flexible scheduling capability on phase φ of node i
$P_{\varphi,i}^{\mathrm{L}}$, $Q_{\varphi,i}^{\mathrm{L}}$	Active/reactive power consumption on phase φ of node i
$E_{\varphi,i}^{\mathrm{EV}}$	Forecasted total charge demand by EV on phase φ of node i
$P_{\varphi,i,t}^{\mathrm{EV,re}}$	Forecasted active power consumption by EV on phase φ of node i at period t
$P_{\varphi,i}^{\mathrm{DG,re}}$	Forecasted active power generated by DG on phase φ of node i
$\bar{Q}_{\varphi,i}^{\mathrm{SOP}}$, $\underline{Q}_{\varphi,i}^{\mathrm{SOP}}$	Upper/lower limit of reactive power provided by SOP on phase φ of node i
L_i^{SOP}	Loss coefficient of SOP at node i
$S_{\varphi,i}^{\mathrm{SOP}}$	Capacity limit of SOP integrated with node i on phase φ
z_{ij}	Impedance matrix of branch ij
A	Symmetric component transformation matrix
S	Phase angle migration diagonal matrix that indicates S= diag(1,e^{j240}, e^{j120})
$\bar{V}_i$, $\underline{V}_i$	Upper/lower voltage limit of node i
$\bar{S}_{ij}$	Upper transmission capacity limit of branch ij
SF_{l-i}^{lp}, SF_{l-i}^{lq}	Sensitivity factors of power flow in branch l to node i
SF_{i-j}^{vp}, SF_{i-j}^{vq}	Sensitivity factors of voltage in node i to node j
LF_i^{P-P}, LF_i^{P-Q}	Active power loss factors of active power/reactive power of node i
LF_i^{P-P}, LF_i^{P-Q}	Reactive power loss factors of active power/reactive power of node i

I. INTRODUCTION

With the increasing environmental pressure, distributed energy resources (DERs) such as electric vehicles (EVs) and distributed generators (DGs) have been widely integrated into distribution networks [1], [2]. Highly volatile DERs not only provide flexible scheduling resources for the optimal operation of low-voltage distribution system, but also put forward new challenges to systems' security, economic operation and energy management.

Low-voltage distribution system has three-phase unbalanced characteristics due to asymmetric three-phase line configuration and large numbers of asymmetric loads. The flexible residential loads represented by EVs and air conditioners usually adopt on-board single-phase charging strategies [3]. The integration of severe unbalanced residential loads may cause inefficient use of network assets, network congestion and voltage violation in low-voltage distribution system. These issues motivate the efforts to propose a congestion management strategy of low-voltage active distribution networks (ADNs) considering the asymmetric access of DERs.

Congestion management methods for distribution networks can be grouped into two categories, including direct regulation methods and market-based methods [4]. In terms of direct regulation, conventional methods such as network reconfiguration and load shedding are considered to solve the congestion problem. But limited by the slow response and security risks due to switching operation, these strategies cannot satisfy the requirement of rapid adjustment with high precision [5]. Soft open point (SOP) is a highly controllable power electronic device installed to replace normally open point, realizing accurate and fast active and reactive power flow control between feeders [6]. The application of SOPs to congestion management of low-voltage ADNs can balance the power flow in different feeders, maximize their regulation potential and further improve the power quality of the system [7], [8].

Though the SOP based congestion management can solve the congestion effectively in many cases, there are some cases where they can only partly solve the congestion due to the limitation of SOP capacities. In such cases, a market mechanism should be considered. Compared with direct regulation methods, market-based methods can efficiently manage and utilize large amounts of DERs, which show great potential in the fields of congestion management. The market-based methods depend on accurate prediction of user's behaviors, thus play a complementary role in congestion management.

For the market-based congestion management methods, a reasonable price signal is the key to stimulate flexible loads to ensure the secure operation of power system. References [9] and [10] proposed the concept of distribution locational marginal price (DLMP) to reflect the congestion cost in distribution networks. In DLMP, EV aggregators respond to the congestion cost and alter their charging plan. Reference [11] considered the effect of reactive power and loss factors on line capacities, a DLMP model based on linearized optimal power flow (OPF) is proposed. In [12], a DLMP congestion management model suited for three-phase systems was built, and phase unbalance limits were modelled in the DC optimal power flow (DCOPF) formulation.

Reference [13] proposed a two-stage congestion management method. Network reconfiguration and OLTC optimization results were obtained through mixed-integer second order-cone programming (MISOCP) modelling. Then, a linear approximation power flow model was built for DLMP calculation. In [14], a dual analysis method was used to analyze the Karush-Kuhn-Tucker condition and DLMP of the second order-cone programming model. The features of various DLMP models are analyzed from the perspectives of computation and numerical precision.

Previous works show the efficiency for handling congestion problems in distribution network. However, most approaches regard three-phase distribution network as a balanced system and use the single-phase equivalent model. Due to the three-phase unbalanced characteristics within the low-voltage distribution system and the single-phase charging strategies in EVs, the results would be inaccurate. Thus, to accurately model the low-voltage ADNs and realize price incentive for the flexible loads in single-phase charging mode, proposing a congestion management strategy of low-voltage ADNs has practical value.

The low-voltage ADNs congestion management is an optimization problem to minimize the operation cost of distribution system operator (DSO) while ensuring the secure operation of the low-voltage network, thus a three-phase power flow model needs to be established. The model, which considers the coupling among phases, involves large numbers of optimization variables. To accelerate computation and enhance the calculation efficiency, the convex relaxation technique has received extensive attention in recent years [15]. Reference [16] proposed a semidefinite programming (SDP) model converted by a three-phase bus-injection model. Low [17] and Gan and Low [18] proved that the bus-injection model and branch-flow model are equivalent in SDP relaxation exactness. The branch-flow based SDP model is numerically more stable because it avoids ill-conditioned operations. Reference [19] combined the SDP model with symmetrical components method to further improve the accuracy of the SDP model under adverse conditions. In [20], a linearized three-phase OPF model considering network loss and voltage violation was proposed, the limitation of the objective function could be overcome. Reference [21] considered a maximum access problem of DG under three-phase linearized OPF model, the approximated linearization method was used to deal with the nonlinear constraints of line capacity. Referring to the state-of-the-art of convex relaxations, congestion management model of low-voltage ADNs can be tractably solved.

The asymmetric access of EVs with high penetration may cause network congestion and voltage issues in low-voltage ADNs. This paper proposes a congestion management method of low-voltage ADNs based on distribution locational marginal price. The main contributions are summarized as follows:

1) A congestion management strategy is presented by combining SOP and market-based mechanisms. The market-based mechanism is invoked in case SOP can't solve the congestion issue. The potential of SOPs and EVs in congestion management is explored to improve the security and operation efficiency of distribution system.
2) The original SOP based congestion management strategy is a highly non-convex nonlinear problem and cannot be efficiently solved. By applying SDP relaxation and symmetrical components method, the original model is converted into a symmetrical SDP model, which can be efficiently solved to meet the demands of large-scale centralized regulation.
3) A three-phase DLMP pricing model for low-voltage ADNs based on sensitivity factors is proposed. The characteristics of three-phase unbalance are considered by linear approximating of low-voltage ADN, which can realize price incentive for the flexible loads in single-phase charging mode. The influence of line congestion, voltage variation, phase-to-phase unbalance and network loss is also considered in the model, which are critical features in ensuring the transmission of real power in low-voltage ADNs operations.

The remainder of this paper is organized as follows. Section II summarizes the framework of congestion management and constructs the congestion management model in low-voltage ADNs. Section III converts the original model to symmetrical SDP form to reduce the computational complexity. The DLMP pricing model based on linearization and sensitivity factors is presented in Section IV. Case studies are given in Section V to verify the effectiveness of the proposed method on the IEEE 33-node and IEEE 123-node low-voltage distribution system. Section VI gives the conclusion of this paper.

II. CONGESTION MANAGEMENT MODELING OF LOW-VOLTAGE ADNs

A. FRAMEWORK OF CONGESTION MANAGEMENT

In our framework of congestion management, DSO solves the problem by coordinating flexible EV loads and SOPs. As a highly controllable power electronic device, SOP can realize power flow regulation and provide reactive power support. On the other hand, flexible charging power of EVs is adjusted by electricity tariff mechanism; that is, DSO handles congestion in a distribution system by employing DLMP to guide EVs to change their charging plan. A congestion management framework of low-voltage ADNs can be deployed as follows:

1) EV aggregators report the EV charging schedules to DSO.

2) Based on the system parameters and operation information, DSOs try to solve the congestion problem with SOPs. A SOP based congestion management model is constructed to optimize the SOP transmitted power. The original problem is then converted to a symmetrical SDP model which can be efficiently solved to meet the demands of rapid centralized control. The system reference operating point can be determined simultaneously.

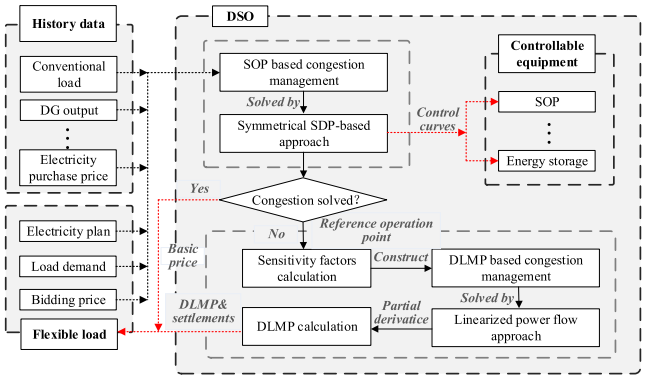

FIGURE 1. Framework of congestion management in low-voltage ADNs.

3) According to the dispatching results, it is judged whether SOPs can completely solve the congestion problem. If all flexible EVs are to charge at the period with the lowest reference purchase price simultaneously, there is no need to adopt DLMP. If not, DLMP is calculated through a DLMP pricing model presented in Step 4) and Step 5).

4) Sensitivity factors are calculated at the reference operating point. A DLMP pricing model is constructed based on the sensitivity factors.

5) The dual variables value of operation constraints can be obtained after solving the DLMP pricing model. The cost of line congestion, including voltage variation, phase-to-phase unbalance and network loss for flexible loads on each phase of every node can be calculated through derivations of Lagrangian function.

B. CONGESTION MANAGEMENT MODELING

1) OBJECTIVE FUNCTION

Accounting for the maximum profits of DSO, the power purchase cost and scheduling cost based on the bidding price of EV are selected as the objective function, which can be formulated as follows:

$$\min f = f^{\text{sub}} + f^{\text{flx}} \tag{1}$$

where the total power purchase cost from higher level electricity grid $f^{\text{sub}}\text{P}_{\text{L,loss}}$ and the scheduling cost for flexible load f^{flx} are formulated as follows:

$$f^{\text{sub}} = \sum_{t=1}^{N_T} \sum_{\varphi=a}^{c} \sigma_t^{\text{r}} P_{\varphi,t}^{\text{sub}} \Delta t \tag{2}$$

$$f^{\text{flx}} = \sum_{t=1}^{N_T} \sum_{i\in\Omega_{\text{EV}}} \sum_{\varphi\in\Phi_i} \sigma_t^{\text{EV}} P_{\varphi,i,t}^{\text{EV,flx}} \Delta t \tag{3}$$

where N_T denotes total periods of the time horizon.

The total power purchase cost f^{sub} can be described as (2), which can be obtained by multiplying the electricity purchase price σ_t^{r} and the purchased electricity quantity $P_{\varphi,t}^{\text{sub}}\Delta t$. $P_{\varphi,t}^{\text{sub}}$ denotes the purchased active power by DSO on phase φ at period t.

In objective function (3), the EV aggregators are assumed to bid at their marginal operation costs σ_t^{EV}. $P_{\varphi,i,t}^{\text{EV,flx}}$ denotes the active power injection by flexible charging EV on phase φ of node i at period t, and Ω_{EV} represents the set of nodes with EV integration.

The constraints include the operation constraints of distribution networks and the operation constraints of the regulation equipment, as described below. For simplicity, the time index is omitted in the following constraints except EVs asymmetric access constraints.

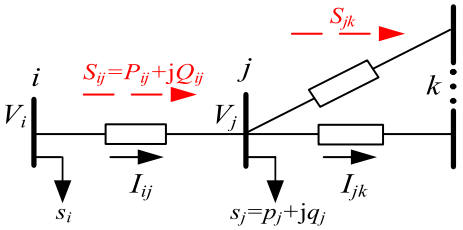

FIGURE 2. Power flows in distribution line segment.

2) SYSTEM OPERATION CONSTRAINTS WITH THREE-PHASE MODELING

Consider the radial distribution networks shown in Fig. 2. The shunt capacitance is ignored since the lines in distribution systems are usually short enough that the admittance can be neglected. The impedance matrix of branch ij is denoted by $z_{ij} = r_{ij}+\text{j}x_{ij}$.

According to Ohm's law, the voltage drop between node i and j can be represented by constraint (4). The sending end voltage V_j can be expressed by the line power flow S_{ij}, $\oslash$ denotes element-wise division. The superscripted asterisk on vectors or matrixes indicates their conjugates, i.e. S_{ij}^*.

$$V_j = V_i - z_{ij}I_{ij} = V_i - z_{ij}(S_{ij}^* \oslash V_j^*) \tag{4}$$

Constraint (5) is the three-phase power balance constraint based on Kirchhoff's law, $\otimes$ denotes element-wise multiplication.

$$\begin{aligned} S_{ij} &= z_{ij}I_{ij}I_{ij}^{\text{H}} + \left(\sum\nolimits_{jk\in\Omega_{\text{b}}} S_{jk}\right) + s_j \\ &= \left(V_i - V_j\right) \otimes i_{ij}^* + \left(\sum\nolimits_{jk\in\Omega_{\text{b}}} S_{jk}\right) + s_j \end{aligned} \tag{5}$$

The security constraints of ADNs are expressed as follows:

$$V_0 = V_0^{\text{ref}} \tag{6}$$

$$\underline{V_i} \le V_i \le \overline{V}_i \tag{7}$$

$$(A^{\text{H}}V_i)(3,1) \le 0.02 \times (A^{\text{H}}V_i)(2,1) \tag{8}$$

$$\sqrt{(P_{ij})^2 + (Q_{ij})^2} \le \overline{S}_{ij} \tag{9}$$

The voltage of source node is fixed and given by constraint (6). V_0^{ref} is assumed as 1.0 p.u., and the angle difference between the three-phase voltage is 120 degrees. Constraint (7) denotes the upper/lower voltage limits at node i. Constraint (8) represents the maximum voltage unbalance factor at node i. The voltage unbalance is defined as the ratio of the negative sequence voltage to the positive sequence voltage. EN50160 standard requires that the negative sequence voltage unbalance of the public connection point should not

exceed 2% in normal operation [22]. $(A^{\mathrm{H}}V_i)(3,1)$ denotes the element of the 3rd row and the first column in the matrix $(A^{\mathrm{H}}V_i)$. The maximum line capacity limit of branch ij is formulated as (9).

3) SOP AND DG OPERATION CONSTRAINTS

$$P_{\varphi,i}^{\mathrm{SOP}} + P_{\varphi,j}^{\mathrm{SOP}} + P_{\varphi,i}^{\mathrm{SOP,loss}} + P_{\varphi,j}^{\mathrm{SOP,loss}} = 0 \tag{10}$$

$$P_{\varphi,i}^{\mathrm{SOP,loss}} = L_i^{\mathrm{SOP}} \sqrt{\left(P_{\varphi,i}^{\mathrm{SOP}}\right)^2 + \left(Q_{\varphi,i}^{\mathrm{SOP}}\right)^2} \tag{11}$$

$$P_{\varphi,j}^{\mathrm{SOP,loss}} = L_j^{\mathrm{SOP}} \sqrt{\left(P_{\varphi,j}^{\mathrm{SOP}}\right)^2 + \left(Q_{\varphi,j}^{\mathrm{SOP}}\right)^2} \tag{12}$$

$$Q_{i,\min}^{\mathrm{SOP}} \le Q_{\varphi,i}^{\mathrm{SOP}} \le Q_{i,\max}^{\mathrm{SOP}}, Q_{j,\min}^{\mathrm{SOP}} \le Q_{\varphi,j}^{\mathrm{SOP}} \le Q_{j,\max}^{\mathrm{SOP}} \tag{13}$$

$$\sqrt{\left(P_{\varphi,i}^{\mathrm{SOP}}\right)^2 + \left(Q_{\varphi,i}^{\mathrm{SOP}}\right)^2} \le S_{\varphi,i}^{\mathrm{SOP}} \tag{14}$$

$$\sqrt{\left(P_{\varphi,j}^{\mathrm{SOP}}\right)^2 + \left(Q_{\varphi,j}^{\mathrm{SOP}}\right)^2} \le S_{\varphi,j}^{\mathrm{SOP}} \tag{15}$$

$$P_{\varphi,i}^{\mathrm{DG}} = P_{\varphi,i}^{\mathrm{DG,re}} \tag{16}$$

$$Q_{\varphi,i}^{\mathrm{DG}} = P_{\varphi,i}^{\mathrm{DG}} \tan\theta_{\varphi,i}^{\mathrm{DG}} \tag{17}$$

This paper uses back-to-back voltage source converters (B2B VSCs) as the realization of SOP, and PQ-V_{dc}Q control is selected as the control mode. Constraint (10) denotes the transmitted active power balance between the two converters. The active power loss of SOP is expressed as (11)-(12), the reactive power constraints and the capacity constraints of SOP are expressed as (13)-(15). Constraints (16)-(17) assume that the active power and the reactive power generated by DGs are equal to the forecasted value.

4) EVS ASYMMETRIC ACCESS CONSTRAINTS

High penetration EVs are considered as a representative of flexible loads which may affect the security and reliability of ADNs. The total charging demand $E_{\varphi,i}^{\mathrm{EV}}$ and the charging power $P_{\varphi,i,t}^{\mathrm{EV,re}}$ are obtained by simulating the EV charging behaviors without considering market influence. The flexible charging constraints of EVs are constructed as follows:

$$\sum_{t=1}^{N_T} P_{\varphi,i,t}^{\mathrm{EV}} \Delta T \ge E_{\varphi,i}^{\mathrm{EV}} \tag{18}$$

$$P_{\varphi,i,t}^{\mathrm{EV}} - P_{\varphi,i,t}^{\mathrm{EV,re}} \ge 0 \quad t \in \Omega_{\mathrm{d}} \tag{19}$$

$$P_{\varphi,i,t}^{\mathrm{EV}} - P_{\varphi,i,t}^{\mathrm{EV,re}} \le 0 \quad t \in \Omega_{\mathrm{e}} \tag{20}$$

$$P_{\varphi,i,t}^{\mathrm{EV,flx}} = 0 \quad t \in \Omega_{\mathrm{d}} \tag{21}$$

$$P_{\varphi,i,t}^{\mathrm{EV,flx}} = P_{\varphi,i,t}^{\mathrm{EV,re}} - P_{\varphi,i,t}^{\mathrm{EV}} \quad t \in \Omega_{\mathrm{e}} \tag{22}$$

$$P_{\varphi,i,t}^{\mathrm{EV}} \ge (1-\alpha_{i,t}) P_{\varphi,i,t}^{\mathrm{EV,re}} \tag{23}$$

Constraint (18) ensures that the total charge power is greater than the charging demand for each EV aggregator. Constraint (19)-(22) assume that flexible charging is only allowed to transfer from the set of on-peak periods Ω_{e} to the set of off-peak periods Ω_{d}. Constraint (23) denotes the lower charging limits at each time.

The original model of SOP based congestion management can be constructed as follows:

$$\begin{aligned} &\text{Origin Model}: \min f = f^{\mathrm{sub}} + f^{\mathrm{flx}} \\ &\text{s.t. } (4) - (23) \end{aligned} \tag{24}$$

Due to the power flow equations and operation constraints of SOPs, the original model (24) is a highly non-convex nonconvex nonlinear programming (NLP) problem, requiring to be solved accurately and efficiently. Hence, in the ensuing section we will discuss how to relax the OPF in (24).

III. SYMMETRICAL SDP MODEL CONVERSION OF CONGESTION MANAGEMENT

As SOPs are directly dispatched by DSO in a centralized manner, it puts forward a strict requirement on the performance of congestion problem solving. In this section, SDP relaxation is adopted to convert the original SOP based congestion management model to a symmetrical SDP model, enabling rapid and accurate calculation.

A. ALTERNATIVE POWER FLOW MODEL

SDP can be mathematically characterized as a type of convex programming, which can be efficiently solved by interior point methods in polynomial time. As SDP offers excellent performance in terms of global optimality, it has been widely used in the optimization of complex systems. On the other hand, SDP model can be more numerically stable and more accurate when adopting symmetrical components method [19]. Symmetrical components method converts the relaxation matrix to positive, negative and zero sequences, which further increases the numerical difference between the matrix elements.

A novel form of system operation constraints is introduced, which can be equivalently described in symmetrical components as follows [19]:

$$\begin{aligned} &\sum\nolimits_{ij\in\Omega_{\mathrm{b}}} \mathrm{diag}\left(A\left(S_{ij}^{012} - z_{ij}^{012} l_{ij}^{012}\right) A^{\mathrm{H}}\right) + s_j \\ &\quad = \sum\nolimits_{jk\in\Omega_{\mathrm{b}}} \mathrm{diag}(A S_{jk}^{012} A^{\mathrm{H}}) \end{aligned} \tag{25}$$

$$\begin{aligned} &\sum\nolimits_{ij\in\Omega_{\mathrm{b}}} \mathrm{diag}\left(A\left(S_{ij}^{012} - z_{ij}^{012} l_{ij}^{012}\right) A^{\mathrm{H}}\right) + s_j \\ &\quad = \sum\nolimits_{jk\in\Omega_{\mathrm{b}}} \mathrm{diag}\left(S_{jk}\right)^{\Phi_j} \end{aligned} \tag{26}$$

$$\begin{aligned} &\sum\nolimits_{ij\in\Omega_{\mathrm{b}}} \mathrm{diag}\left(S_{ij} - z_{ij} l_{ij}\right) + s_j \\ &\quad = \sum\nolimits_{jk\in\Omega_{\mathrm{b}}} \mathrm{diag}\left(S_{jk}\right)^{\Phi_j} \end{aligned} \tag{27}$$

$$\begin{aligned} s_i = p_{\varphi,i} + \mathrm{j}q_{\varphi,i} &= \left(P_{\varphi,i}^{\mathrm{DG}} + \mathrm{j}Q_{\varphi,i}^{\mathrm{DG}}\right) + \left(P_{\varphi,i}^{\mathrm{SOP}} + \mathrm{j}Q_{\varphi,i}^{\mathrm{SOP}}\right) \\ &\quad - \left(P_{\varphi,i}^{\mathrm{L}} + \mathrm{j}Q_{\varphi,i}^{\mathrm{L}}\right) - P_{\varphi,i}^{\mathrm{EV}} \end{aligned} \tag{28}$$

$$v_i^{012} - v_j^{012} - \left(S_{ij}^{012} z_{ij}^{012,\mathrm{H}} + z_{ij}^{012} S_{ij}^{012,\mathrm{H}}\right) + z_{ij}^{012} l_{ij}^{012} z_{ij}^{012,\mathrm{H}} = 0 \tag{29}$$

$$\begin{bmatrix} v_i^{012} & S_{ij}^{012} \\ S_{ij}^{012,\mathrm{H}} & l_{ij}^{012} \end{bmatrix} \ge 0 \tag{30}$$

$$\text{rank}\begin{bmatrix} v_i^{012} & S_{ij}^{012} \\ S_{ij}^{012,\mathrm{H}} & l_{ij}^{012} \end{bmatrix} = 1 \tag{31}$$

$$(v_i)^{\Phi_j} - v_j - \left(S_{ij} z_{ij}^{\mathrm{H}} + z_{ij} S_{ij}^{\mathrm{H}}\right) + z_{ij} l_{ij} z_{ij}^{\mathrm{H}} = 0 \tag{32}$$

$$\begin{bmatrix} (v_i)^{\Phi_j} & S_{ij} \\ S_{ij}^{\mathrm{H}} & l_{ij} \end{bmatrix} \geq 0 \tag{33}$$

$$\text{rank}\begin{bmatrix} (v_i)^{\Phi_i} & S_{ij} \\ S_{ij}^{\mathrm{H}} & l_{ij} \end{bmatrix} = 1 \tag{34}$$

Constraints (25)-(27) represent the complex power balance of node i in the sequence network, which applies to three-phase nodes. When the downstream branch jk is a three-phase line, the power balance constraint is described as (25). When the branch jk is a single-phase or two-phase line, the power balance constraint is described as (26). For single-phase or two-phase cases of node i, the power flow balance constraint is described as (27).

The active power injection $p_{\varphi,i}$ and reactive power injection $q_{\varphi,i}$ on phase φ of node i can be described as (28). Constraint (29) represents Ohm's law of branch ij in sequence network which applies to three-phase branches. Constraints (30) and (31) indicate the positive semidefinite constraint and the rank-one constraint of the matrix variable for three-phase branches. In single-phase or two-phase cases, Ohm's law, the positive semidefinite constraint and the rank-one constraint are described as (32)-(34).

The security constraints of ADNs in auxiliary variables form with symmetrical components are expressed as follows:

$$v_0^{012} = V_0^{012,\mathrm{ref}} \left(V_0^{012,\mathrm{ref}}\right)^{\mathrm{H}} \tag{35}$$

$$\left(\underline{V_i}\right)^2 \leq \mathrm{diag}\left(A v_i^{012} A^{\mathrm{H}}\right) \leq \left(\overline{V}_i\right)^2 \tag{36}$$

$$v_i^{012}(3,3) \leq 0.02^2 \times \left(v_i^{012}(2,2)\right) \tag{37}$$

$$\sqrt{\left(\mathrm{real}\left(A S_{ij}^{012} A^{\mathrm{H}}\right)\right)^2 + \left(\mathrm{imag}\left(A S_{ij}^{012} A^{\mathrm{H}}\right)\right)^2} \leq \overline{S}_{ij} \tag{38}$$

The voltage auxiliary variables of source node in symmetrical components are given by constraint (35), where $V_0^{012,\mathrm{ref}} = A^{\mathrm{H}}\left[1 \ \mathrm{e}^{\mathrm{j}240} \ \mathrm{e}^{\mathrm{j}120}\right]$.

By introducing the novel form of system operation constraints, the SOP based congestion management model is convex except for (11)-(12), (14)-(15), (31), (34), (38). An SDP relaxation is adopted to convert the model to a symmetrical SDP model.

B. CONVERSION TO SYMMETRICAL SDP MODEL

A symmetrical SDP model is adopted in this step, enabling rapid and accurate calculation. The conversion procedure is elaborated as follows.

1) Semidefinite relaxation can be obtained by removing the rank-one constraints (31) and (34) due to their non-convex characteristic.

2) Note that constraint (38) is a convex quadratic constraint, which is a special case of SDP, and it can be replaced by constraint (39)-(41) in SDP form.

$$P_{ij} = \mathrm{real}\left(A S_{ij}^{012} A^{\mathrm{H}}\right) \tag{39}$$

$$Q_{ij} = \mathrm{imag}\left(A S_{ij}^{012} A^{\mathrm{H}}\right) \tag{40}$$

$$\begin{bmatrix} \overline{S_{\varphi,ij}} & P_{\varphi,ij} + \mathrm{j}Q_{\varphi,ij} \\ P_{\varphi,ij} - \mathrm{j}Q_{\varphi,ij} & \overline{S_{\varphi,ij}} \end{bmatrix} \geq 0 \tag{41}$$

3) The SOP and DG operation constraints (11), (12), (14) and (15) are convex quadratic constraints, a similar method can be used to convert them to SDP form:

$$\begin{bmatrix} S_{\varphi,i}^{\mathrm{a}} & P_{\varphi,i}^{\mathrm{a}} - \mathrm{j}Q_{\varphi,i}^{\mathrm{a}} \\ P_{\varphi,i}^{\mathrm{a}} + \mathrm{j}Q_{\varphi,i}^{\mathrm{a}} & S_{\varphi,i}^{\mathrm{a}} \end{bmatrix} \geq 0, \quad \mathrm{a} \in \{\mathrm{SOP}, \mathrm{DG}\} \tag{42}$$

$$\begin{bmatrix} P_{\varphi,i}^{\mathrm{SOP,loss}}/L_i^{\mathrm{SOP}} & P_{\varphi,i}^{\mathrm{SOP}} - \mathrm{j}Q_{\varphi,i}^{\mathrm{SOP}} \\ P_{\varphi,i}^{\mathrm{SOP}} + \mathrm{j}Q_{\varphi,i}^{\mathrm{SOP}} & P_{\varphi,i}^{\mathrm{SOP,loss}}/L_i^{\mathrm{SOP}} \end{bmatrix} \geq 0 \tag{43}$$

$$\begin{bmatrix} P_{\varphi,j}^{\mathrm{SOP,loss}}/L_j^{\mathrm{SOP}} & P_{\varphi,j}^{\mathrm{SOP}} - \mathrm{j}Q_{\varphi,j}^{\mathrm{SOP}} \\ P_{\varphi,j}^{\mathrm{SOP}} + \mathrm{j}Q_{\varphi,j}^{\mathrm{SOP}} & P_{\varphi,j}^{\mathrm{SOP,loss}}/L_j^{\mathrm{SOP}} \end{bmatrix} \geq 0 \tag{44}$$

Then the original model (24) can be reformulated to the relaxed SDP model as follows.

$$\begin{aligned} &\text{SDP Model}: \ \min f = f^{\mathrm{sub}} + f^{\mathrm{flx}} \\ &\text{s.t. } (10), (13), (16) - (23), (25) - (30), \\ &\quad (32) - (33), (35) - (37), (39) - (44) \end{aligned} \tag{45}$$

The optimal operation model (45) based on symmetrical SDP form is obtained which can be efficiently solved by existing algorithm package. To quantify the exactness of SDP relaxation, the two largest eigenvalues of matrix variables λ_1 and λ_2 ($|\lambda_1| \geq |\lambda_2| \geq 0$) are calculated and the ratio $= |\lambda_2/\lambda_1|$ is obtained. The smaller ratio indicates the matrix variable to rank one is closer. By solving the above model, optimal scheme of SOP and the reference operating point of the system can be obtained.

DSO usually can't directly dispatch the charging behaviors of EV. Thus, if the congestion still exists, a DLMP pricing model for low-voltage ADNs is needed to motivate EV aggregators to solve congestion problem. Because it is difficult to calculate DLMP directly in SDP model through duality analysis, a novel DLMP pricing model based on node injection power sensitivity is proposed.

IV. DLMP PRICING MODEL CONVERSION OF CONGESTION MANAGEMENT

In this section, the sensitivity factors in three-phase system are calculated by linearization. Then, a DLMP pricing model based on sensitivity factor is presented, which helps to disperse the EV's charging demands to a lighter loading period.

A. SENSITIVITY FACTORS CALCULATION

1) LINEARIZED POWER FLOW MODEL

Compared with the original model of SOP based congestion management in (24), the original DLMP pricing model

remove the operation constraints of SOP and DG. The original DLMP pricing model is still nontrivial due to the nonlinear terms in the power flow constraints. Moreover, the decision variables in this model involve the active power flow P_{ij} and the reactive power flow Q_{ij}. To facilitate the calculation of DLMP, the original model is reformulated as a sensitivity based linearization model.

Linear approximation is considered in the DLMP pricing model which can be used to remove the non-convexity and nonlinearity of constraints (4)-(5). Because the variation of the nodal voltage V_i is small, the voltage drop is nearly linear around the desired operating point [20], [21]. The voltage variable V_j^* in Eq. (4) is approximated to a constant near the reference operating point which can be obtained by the symmetrical SDP model. The branch impedance z_{ij} is replaced by $\hat{r}_{ij}$ and $\hat{x}_{ij}$ which can be formulated as follows:

$$V_j \approx V_i - \left(\hat{r}_{ij} + \hat{x}_{ij}\right)(P_{ij} - \mathrm{j}Q_{ij}) \tag{46}$$

$$\hat{r}_{ij} = \mathrm{real}(\bar{a}_i \bar{a}_i^{\mathrm{H}}) r_{ij} - \mathrm{j}(\mathrm{imag}\left(\bar{a}_i \bar{a}_i^{\mathrm{H}}\right) x_{ij}) \tag{47}$$

$$\hat{x}_{ij} = \mathrm{real}(\bar{a}_i \bar{a}_i^{\mathrm{H}}) x_{ij} + \mathrm{j}(\mathrm{imag}\left(\bar{a}_i \bar{a}_i^{\mathrm{H}}\right) r_{ij}) \tag{48}$$

$$\bar{a}_i = \left[\, \mathrm{e}^{-\mathrm{j}\theta_{ia}} \ \mathrm{e}^{-\mathrm{j}\theta_{ib}} \ \mathrm{e}^{-\mathrm{j}\theta_{ic}} \,\right]^{\mathrm{T}} \oslash V_i^{rf} \tag{49}$$

$$S_{ij}^{\mathrm{loss}} = \left(V_i - V_j\right) \otimes i_{ij}^* = [S_{ij} \oslash V_i][z_{ij}(S_{ij}^* \oslash V_j^*)] \tag{50}$$

$$S_{ij}^{\mathrm{loss}} \approx [P_{ij} + \mathrm{j}Q_{ij}][\left(\hat{r}_{ij} + \hat{x}_{ij}\right)(P_{ij} - \mathrm{j}Q_{ij})] \tag{51}$$

Equation (46) represents the linearized Ohm's law of the branch. $\hat{r}_{ij}$ and $\hat{x}_{ij}$ can be calculated using equations (47)-(49), where V_i^{rf} denotes the voltage of node i at the reference operating point. The nonlinear network loss item in equation (5) can be rewritten as (50). Similar method is considered to eliminate V_j^* in equation (50), which can be represented as equation (51). Note that equation (51) is nonlinear, it can be linearized by calculating the loss sensitivity factors around the operating point.

2) SENSITIVITY FACTORS OF BRANCH FLOW, VOLTAGE AND NETWORK LOSS

The relationship between branch flow, nodal voltage, active power loss and node injection power are analyzed to obtain the sensitivity factors, which will help to facilitate the calculation of DLMP.

To solve the problem of line congestion, the power transfer factors are used to establish the linear relationship between line power flow and node injection power. Considering that loss term is much smaller than the branch power flow, we first consider the situation without network loss, which can be formulated as follows:

$$\begin{bmatrix} P_{ij}^a + \mathrm{j}Q_{ij}^a \\ P_{ij}^b + \mathrm{j}Q_{ij}^b \\ P_{ij}^c + \mathrm{j}Q_{ij}^c \end{bmatrix} \approx \begin{bmatrix} M^a & & \\ & M^b & \\ & & M^c \end{bmatrix} \begin{bmatrix} P_{\mathrm{inj}}^a + \mathrm{j}Q_{\mathrm{inj}}^a \\ P_{\mathrm{inj}}^b + \mathrm{j}Q_{\mathrm{inj}}^b \\ P_{\mathrm{inj}}^c + \mathrm{j}Q_{\mathrm{inj}}^c \end{bmatrix} \tag{52}$$

For the cases neglecting network loss, the branch power flow in the asymmetric network can be decomposed into three independent networks A, B, and C. The branch power flow of each phase is approximately equal to the sum of the injected power of the nodes downstream of each phase. Thus, the sensitivity factors of branch flow can be written as:

$$SF_{l-i}^{lp} = \frac{\partial P_l^f}{\partial P_i^{\mathrm{inj}}} = \mathrm{diag}(\, M_{l-i}^a \ M_{l-i}^b \ M_{l-i}^c \,) \tag{53}$$

$$SF_{l-i}^{lq} = \frac{\partial Q_l^f}{\partial Q_i^{\mathrm{inj}}} = \mathrm{diag}(\, M_{l-i}^a \ M_{l-i}^b \ M_{l-i}^c \,) \tag{54}$$

Based on the linearized Ohm's law of branch in equation (12), the relationship between nodal voltage and injected power is analyzed and linearized. Then, the voltage sensitivity factors are deduced. The branch active power P_{ij} and the reactive power Q_{ij} can be represented as P_{inj} and Q_{inj} through equation (52). Thus, the voltage sensitivity factors can be obtained by calculating the partial derivative of the node injection power, which can be formulated as:

$$SF_{i-j}^{vp} = \frac{\partial (V_0 - V_i)}{\partial P_i^{\mathrm{inj}}} = \begin{bmatrix} Dpv_{i-j}^{a-a}(1,1) & Dpv_{i-j}^{a-b}(1,2) & Dpv_{i-j}^{a-c}(1,3) \\ Dpv_{i-j}^{b-a}(2,1) & Dpv_{i-j}^{b-b}(2,2) & Dpv_{i-j}^{b-c}(2,3) \\ Dpv_{i-j}^{c-a}(3,1) & Dpv_{i-j}^{c-b}(3,2) & Dpv_{i-j}^{c-c}(3,3) \end{bmatrix} \tag{55}$$

$$SF_{i-j}^{vq} = \frac{\partial (V_0 - V_i)}{\partial Q_i^{\mathrm{inj}}} = \begin{bmatrix} Dqv_{i-j}^{a-a}(1,1) & Dqv_{i-j}^{a-b}(1,2) & Dqv_{i-j}^{a-c}(1,3) \\ Dqv_{i-j}^{b-a}(2,1) & Dqv_{i-j}^{b-b}(2,2) & Dqv_{i-j}^{b-c}(2,3) \\ Dqv_{i-j}^{c-a}(3,1) & Dqv_{i-j}^{c-b}(3,2) & Dqv_{i-j}^{c-c}(3,3) \end{bmatrix} \tag{56}$$

where $Dpv_{i-j}^{\varphi_1-\varphi_2}(X,Y)$, $Dqv_{i-j}^{\varphi_1-\varphi_2}(X,Y)$, $\check{r}_{ij}$ and $\check{x}_{ij}$ satisfy:

$$Dpv_{i-j}^{\varphi_1-\varphi_2}(X,Y) = \sum\nolimits_{l\in\Omega_b} M_{l-i}^{\varphi_1} M_{l-j}^{\varphi_2} \check{r}_l(X,Y) + \mathrm{j}\sum\nolimits_{l\in\Omega_b} M_{l-i}^{\varphi_1} M_{l-j}^{\varphi_2} \check{x}_l(X,Y) \tag{57}$$

$$Dqv_{i-j}^{\varphi_1-\varphi_2}(X,Y) = \sum\nolimits_{l\in\Omega_b} M_{l-i}^{\varphi_1} M_{l-j}^{\varphi_2} \check{x}_l(X,Y) - \mathrm{j}\sum\nolimits_{l\in\Omega_b} M_{l-i}^{\varphi_1} M_{l-j}^{\varphi_2} \check{r}_l(X,Y) \tag{58}$$

$$\check{r}_l = \mathrm{real}\left(\hat{r}_l\right) - \mathrm{imag}\left(\hat{x}_l\right) \tag{59}$$

$$\check{x}_l = \mathrm{real}(\hat{x}_l) + \mathrm{imag}(\hat{x}_l) \tag{60}$$

The voltage sensitivity factors are series of complex matrices which can reflect the effect on both magnitude and angles.

The nonlinear network loss item in (51) is a second-order equation, we first use equation (52) to replace branch active power P_{ij} and reactive power Q_{ij} to P_{inj} and Q_{inj}. Then, the network loss derivative of the node injection power at the reference operating point is calculated. $P_l^{\varphi,rf}$ is introduced to

replace P_l^{φ}, thus, the loss factors are deduced as follows:

$$LF_i^{P-P} = \sum_{l\in\Omega_b} \frac{\partial P_{l,\text{loss}}}{\partial P_i^{\text{inj}}} = f\left(M_{l-i}^{\varphi}, P_l^{\varphi,rf}, \hat{r}_l\right) = \sum_{l\in\Omega_b} \text{diag}\begin{bmatrix} M_{l-i}^{a}\left(2P_l^{a,rf}\hat{r}_l(1,1)+P_l^{b,rf}\hat{r}_l(1,2)+P_l^{c,rfg}\hat{r}_l(1,3)\right) \\ M_{l-i}^{b}\left(P_l^{a,rf}\hat{r}_l(2,1)+2P_l^{b,rf}\hat{r}_l(2,2)+P_l^{c,rf}\hat{r}_l(2,3)\right) \\ M_{l-!i}^{c}\left(P_l^{a,rf}\hat{r}_l(3,1)+P_l^{b,rf}\hat{r}_l(3,2)+2P_l^{c,rf}\hat{r}_l(3,3)\right) \end{bmatrix}^{\text{T}} \begin{bmatrix} 0 & M_{l-i}^{b}P_l^{a,rf}\hat{r}_l(2,1) & M_{l-i}^{c}P_l^{a,rf}\hat{r}_l(3,1) \\ M_{l-i}^{a}P_l^{b,rf}\hat{r}_l(1,2) & 0 & M_{l-i}^{c}P_l^{b,rf}\hat{r}_l(3,2) \\ M_{l-i}^{a}P_l^{c,rf}\hat{r}_l(1,3) & M_{l-i}^{b}P_l^{c,rf}\hat{r}_l(2,3) & 0 \end{bmatrix} \tag{61}$$

where $P_l^{\varphi,rf}$ represents the branch flow value at the reference operating point of the system and is calculated from the SDP model. Similarly, LF_i^{P-Q}, LF_i^{Q-Q} and LF_i^{Q-P} can be introduced to characterize the factors between active network loss and reactive power, reactive power loss and reactive power, reactive power loss and active power, respectively. The general calculating formulas can be written as:

$$LF_i^{P-Q} = \sum_{l\in\Omega_b} \frac{\partial P_{l,\text{loss}}}{\partial Q_i^{\text{inj}}} = f(M_{l-i}^{\varphi}, Q_l^{\varphi,rf}, \hat{r}_l) \tag{62}$$

$$LF_i^{Q-Q} = \sum_{l\in\Omega_b} \frac{\partial Q_{l,\text{loss}}}{\partial Q_i^{\text{inj}}} = f(M_{l-i}^{\varphi}, Q_l^{\varphi,rf}, \hat{x}_l) \tag{63}$$

$$LF_i^{Q-P} = \sum_{l\in\Omega_b} \frac{\partial Q_{l,\text{loss}}}{\partial P_i^{\text{inj}}} = f(M_{l-i}^{\varphi}, P_l^{\varphi,rf}, \hat{x}_l) \tag{64}$$

The above derivation process does not consider the effect of network loss on branch flow sensitivity factors and voltage sensitivity factors. To improve the accuracy of the congestion management model, the concept of fictitious nodal demand is introduced [23]. The basic idea is to divide the power loss in a line into two equal power injections to the two nodes of the line. The node active network loss F_i^P and the reactive network loss F_i^Q can be formulated as:

$$F_i^P = \frac{1}{2}\sum_{j\in N(i)} r_{ij}[\left(P_{ij}^{rf}\right)^2 + \left(Q_{ij}^{rf}\right)^2] \oslash \left(U_i^{rf}\right)^2 \tag{65}$$

$$F_i^Q = \frac{1}{2}\sum_{j\in N(i)} x_{ij}[\left(P_{ij}^{rf}\right)^2 + \left(Q_{ij}^{rf}\right)^2] \oslash \left(U_i^{rf}\right)^2 \tag{66}$$

where U_i^{rf} denotes the voltage magnitude of node i in the reference operating point.

B. DLMP PRICING MODEL

Based on the sensitivity factors of branch flow, voltage and network loss, a DLMP pricing model is constructed. EV aggregators are considered in the model. Through the pricing model, DLMP can be calculated to guide EV aggregators to improve network loss, voltage quality, three-phase unbalance, line overload conditions in low-voltage distribution systems. To facilitate the calculation of DLMP, the original model is reformulated as a sensitivity factors based linearization model. The procedure of conversion is elaborated as follows.

The three-phase system operation constraints are reformulated as follows:

$$P^{\text{sub}} + \sum_{i\in N}\left(1 - LF_i^{P-P}\right)P_i^{\text{inj}} + \sum_{i\in N} LF_i^{P-Q}Q_i^{\text{inj}} + P_{\text{loss}}^{\text{r}} = 0(\lambda_p) \tag{67}$$

$$Q^{\text{sub}} + \sum_{i\in N}\left(1 - LF_i^{Q-Q}\right)Q_i^{\text{inj}} + \sum_{i\in N} LF_i^{Q-P}P_i^{\text{inj}} + Q_{\text{loss}}^{\text{r}} = 0(\lambda_q) \tag{68}$$

$$P_i^{\text{inj}} = P_i^{\text{DG}} + P_i^{\text{SOP,r}} - P_i^{\text{EV}} - P_i^{\text{L}} \tag{69}$$

$$Q_i^{\text{inj}} = Q_i^{\text{DG}} + Q_i^{\text{SOP,r}} - Q_i^{\text{L}} \tag{70}$$

$$V_i = V_0 - \sum_{i\in N} SF_{i-j}^{vp}\left(P_i^{\text{inj}} + F_i^P\right) - \sum_{i\in N} SF_{i-j}^{vq}(Q_i^{\text{inj}} + F_i^Q) \tag{71}$$

Constraints (67)-(68) represent the active power and reactive power balance based on network loss sensitivity, which can be used to calculate active power and reactive power in the source node. The loss cost of each node can be obtained through derivations of the Lagrangian function. $P_i^{\text{SOP,r}}$ and $Q_i^{\text{SOP,r}}$ denote active power and reactive power of SOPs under the reference operating point. $P_{\text{loss}}^{\text{r}}$ and $Q_{\text{loss}}^{\text{r}}$ are the system network active power loss and reactive power loss optimized through SDP model. Constraint (71) represents the voltage variation based on voltage sensitivity factors.

The security constraints of ADNs (6)-(9) are reformulated as follows:

$$\underline{V_i} \le \text{real}(V_0) - \sum_{i\in N}\text{real}\left(\text{S}\cdot SF_{i-j}^{vp}\right)\left(P_i^{\text{inj}} + F_i^P\right) - \sum_{i\in N}\text{real}\left(\text{S}\cdot SF_{i-j}^{vq}\right)\left(Q_i^{\text{inj}} + F_i^Q\right)(\mu_i^-) \tag{72}$$

$$\alpha_{c,0}\text{real}(V_i) + \alpha_{c,1}\text{imag}(V_i) + \alpha_{c,2}\overline{V}_i \le 0(\mu_i^+) \tag{73}$$

$$\alpha_{c,0}V_i^{\text{sym,real}}(3,1) + \alpha_{c,1}V_i^{\text{sym,imag}}(3,1) + 0.02\cdot\alpha_{c,2}V_i^{\text{sym,real}}(2,1) \le 0(\mu_{i,\text{unb}}) \tag{74}$$

$$V_i^{\text{sym,real}} = \text{real}\left(A^{\text{H}}V_i\right) \tag{75}$$

$$V_i^{\text{sym,imag}} = \text{imag}\left(A^{\text{H}}V_i\right) \tag{76}$$

$$\alpha_{c,0}\sum_{i\in N} SF_{l-i}^{lp}(P_i^{\text{inj}} + F_i^P) + \alpha_{c,1}\sum_{i\in N} SF_{l-i}^{lp}(Q_i^{\text{inj}} + F_i^Q) + \alpha_{c,2}\overline{S}_{ij} \le 0(\omega_{l,c}) \tag{77}$$

Constraints (72)-(73) denote the lower/upper voltage limits of node i which can be used to calculate the voltage magnitude cost. The boundary of voltage magnitude tolerance can be depicted as follows:

As shown in Fig. 3, the boundary of voltage magnitude tolerance is limited in the red region. Considering the actual situation that the voltage phase deviation is small, the accuracy of the linearized approximation can be guaranteed. A polygonal inner-approximation method is considered, where $\alpha_{c,0}$, $\alpha_{c,1}$, and $\alpha_{c,2}$ are the coefficients used to describe the polygonal approximation [24].

Constraints (74)-(76) represent the maximum voltage unbalance in node i. The maximum line capacity limit of branch ij is formulated as (77).

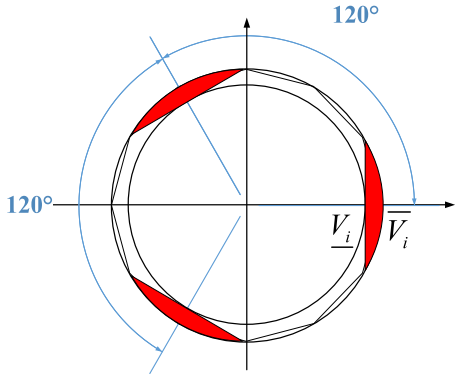

FIGURE 3. Boundary of voltage magnitude tolerance in phase plane.

Thus, the original model on the reference operating point can be reformulated to the linearized model without considering SOP and DG operation constraints.

$$\begin{aligned} &\text{Linearized Model}: \ \min f = f^{\text{sub}} + f^{\text{flx}} \\ &\text{s.t. } (18)-(23),(67)-(77) \end{aligned} \tag{78}$$

By differentiating Lagrangian function, the above model can be easily transformed into an unconstrained optimization model. DLMP at each node in each phase can be calculated through the first-order partial derivative which can be formulated as follows:

$$\sigma_i^P = \sigma_t^{\text{r}} + \sigma_i^{\text{c}} + \sigma_i^{\text{vol}} + \sigma_i^{\text{los}} \tag{79}$$

By adopting linearized model, DLMP can be decomposed into electricity purchase price, congestion price σ_i^{c}, voltage price σ_i^{vol}, and loss price σ_i^{los}. Unlike the cases in the balanced model, π_i^P denotes $\pi_i^P := (\pi_{\varphi,i}, \varphi \in \Phi_{ij}) \in R^{|3|}$ with the missing phase filled with zeros. The specific forms of each part can be formulated as follows:

$$\sigma_i^{\text{c}} = \sum\nolimits_{l\in\Omega_{\text{b}}} \sum\nolimits_c \alpha_{c,0} SF_{lp,l-i}\omega_{l,c} \tag{80}$$

$$\sigma_i^{\text{vol}} = \sigma_i^{\text{vol,mag}} + \sigma_i^{\text{vol,unb}} \tag{81}$$

$$\begin{aligned} \sigma_i^{\text{vol,mag}} &= \text{diag}(\sum\nolimits_{j\in\text{N}} \text{real}(\text{S}\cdot(SF_{j-i}^{vp})^{\text{T}}))\mu_i^- \\ &+ \text{diag}(\sum\nolimits_{j\in\text{N}} \text{imag}(\text{S}\cdot(SF_{j-i}^{vp})^{\text{T}})\mu_i^- \\ &+ \sum\nolimits_{j\in\text{N}} \sum\nolimits_c (\alpha_{c,0}\text{real}((SF_{j-i}^{vp})^{\text{T}}))\mu_i^+ \\ &+ \sum\nolimits_{j\in\text{N}} \sum\nolimits_c (\alpha_{c,1}\text{imag}((SF_{j-i}^{vp})^{\text{T}}))\mu_i^+ \end{aligned} \tag{82}$$

$$\begin{aligned} \sigma_i^{\text{vol,unb}} &= \text{diag}(\sum\nolimits_{j\in\text{N}} \text{real}(A_3 \times (SF_{j-i}^{vp})^{\text{T}}))\mu_{i,\text{unb}} \\ &+ \text{diag}(\sum\nolimits_{j\in\text{N}} \text{imag}(A_3 \times (SF_{j-i}^{vp})^{\text{T}}))\mu_{i,\text{unb}} \\ &+ \text{diag}(0.02 \cdot \sum\nolimits_{j\in\text{N}} \text{real}(A_2 \times (SF_{j-i}^{vp})^{\text{T}}))\mu_{i,\text{unb}} \end{aligned} \tag{83}$$

$$\sigma_i^{\text{los}} = (LF_i^{P-P})^{\text{T}}\lambda_p + (LF_i^{Q-P})^{\text{T}}\lambda_q \tag{84}$$

where μ_i^- and μ_i^+ denote the dual variables of constraints (72)-(73), satisfying $\mu_i^-, \mu_i^+ \in R^{|3|}$. The lower/upper voltage limits in phases A, B and C are extended to the first, second and third columns respectively and the elements are equal in each column. $\mu_{i,\text{unb}}$ and $\omega_{l,c}$ denote the dual variables of constraints (74) and (77), satisfying $\mu_{i,\text{unb}}, \omega_{l,c} \in R^{|3|}$. A_2 and A_3 denote the second/third row of the symmetric component transformation matrix.

In summary, the original flexible load pricing model is converted to a large-scale linear optimization model that can be efficiently solved based on the interior point method. The dual variables can be obtained simultaneously.

V. CASE STUDIES AND ANALYSIS

In this section, the modified IEEE 33-node and IEEE 123-node three-phase distribution system are used to demonstrate the effectiveness and efficiency of the proposed method. The proposed method is implemented in the YALMIP optimization toolbox [25] with MATLAB R2013a, and solved by MOSEK 7.1.0.14. The simulations are carried out on a computer with an Intel(R) Core(TM) i5-3470 at 3.20 GHz with 8 GB RAM.

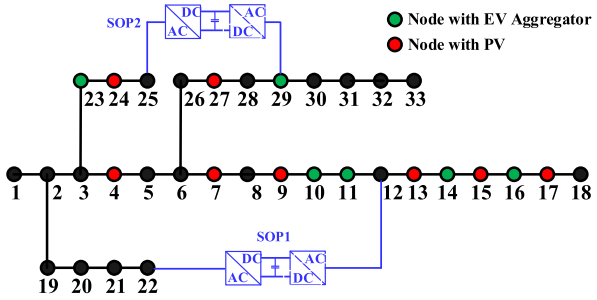

FIGURE 4. Structure of the modified IEEE 33-node system.

A. THE MODIFIED IEEE 33-NODE SYSTEM

1) SYSTEM PARAMETER SETTING

As shown in Fig. 4, the test system is a modified IEEE 33-node distribution system [26], of which the unbalanced branch and load data are from [27]. The total active and reactive loads of the system are 3635 kW and 2265 kvar, respectively. The red nodes are the locations that integrated with photovoltaic generators (PVs). Eight asymmetric access PVs are integrated and operate with a constant power factor of 0.95.

The green nodes are the locations that integrated with EV aggregators. Six EV aggregators are integrated into the networks in single-phase charging mode. The EV aggregators' charging plan without considering market influence is obtained through Monte Carlo simulations, which is presented in [28]. The detailed parameters are provided in [29]. The simulation result of the EV aggregators with fifty EVs is shown in Fig. 5.

The basic installation parameters are shown in TABLE 1 and TABLE 2.

To replace the tie switch in the distribution network, two groups of SOPs with a capability of 500 kVA are installed between nodes 12 and 22, as well as the nodes 25 and 29,

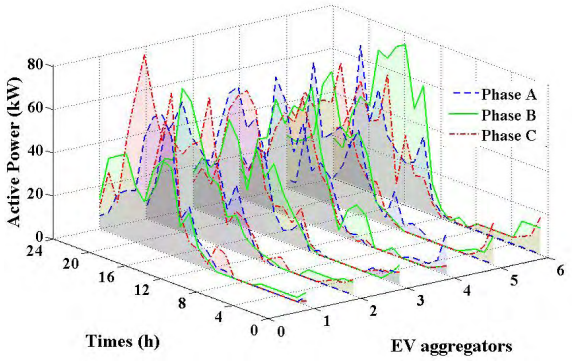

FIGURE 5. Charging plans of EV aggregator with fifty EVs in Case 3 and Case 4.

TABLE 1. Basic installation parameters of DGs.

Parameter	Photovoltaic cells							
Location	4	7	9	13	15	17	24	27
Phase	C	C	B	A	B	C	B	C
Capacity (kVA)	200	300	300	150	300	150	150	200

TABLE 2. Basic installation parameters of EV aggregators.

Parameter	EV aggregators					
Location	10	11	14	16	23	29
Phase	ABC	ABC	ABC	ABC	ABC	ABC

TABLE 3. Configuration of line capacity limitation.

Branch power flow limitation (kVA)	Branch power flow in normal operation (kVA)
500	<300
800	300–500
1500	>500

of which the upper reactive power limit on each phase is 300 kvar. It is assumed that the loss coefficient of each SOP is 0.02. The limitation of system voltage is set to 0.95 p.u. and 1.05 p.u., respectively. The on-peak periods Ω_e are set as 0 am to 6 am in this paper.

In distribution networks, the branches near the substation have larger line capacities than those far from the substation. Based on the branch power flow in normal operation [30], the line capacities of the branches are listed in Table 3.

In order to verify the effectiveness of SOPs and DLMP in congestion management, four scenarios are adopted to analyze the performance of the congestion management method.

Case 1: The initial operation state of unbalanced ADNs without any congestion management. Six EV aggregators are integrated into the networks in single phase charging mode and each phase is integrated with twenty-five EVs. Flexible EVs are to charge at the period with the lowest electricity purchase price.

Case 2: DSO uses SOPs to solve the congestion problem. Each EV aggregator is integrated with twenty-five EVs in each phase and flexible EVs are to charge at the period with the lowest electricity purchase price.

Case 3: DSO uses SOPs to solve the congestion problem. Each EV aggregator is integrated with fifty EVs in each phase and flexible EVs are to charge at the period with the lowest electricity purchase price.

Case 4: DSO uses both SOPs and DLMP to solve the congestion problem, DLMPs are delivered to the EV aggregators, which incentivize the EVs to contribute to system operation based on the price signals. Each EV aggregator is integrated with fifty EVs in each phase.

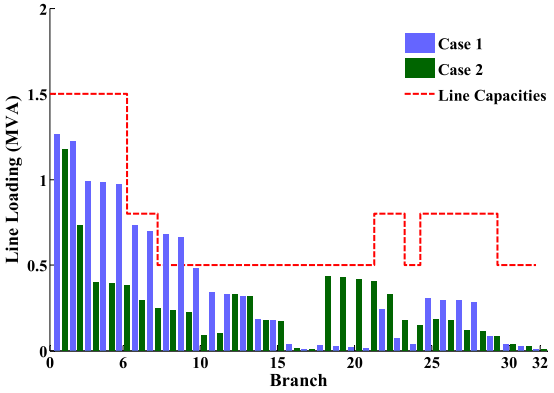

FIGURE 6. Load level of distribution line in Case1 and Case 2.

2) RESULTS AND ANALYSIS OF SOP BASED CONGESTION MANAGEMENT

Case 1 and Case 2 are selected to verify the effectiveness of SOPs in congestion management. As shown in Fig. 6, a ladder-like line capacity constraint is considered by the red dotted line [30], thus, congestion may occur in any branch.

The bar represents the heaviest phase loading of the three-phase line. Branches 8 and 9 appear congestion problem in Case 1 and the power flow on branch 8 exceeds 20% of the line capacity limits. In Case 2, with the access of SOPs between nodes 12 and 22, SOPs help supply the load on nodes 12-18, thus eliminating the congestion problem.

Fig. 7 shows the three-phase voltage profile in Case 1 and 2 during period 3. The three-phase reactive power outputs of SOPs locally compensate the reactive power demands, avoiding the remote transmission of reactive power from sources. Thus, the reactive power support of SOPs can effectively improve the voltage profile.

The SOP-based congestion management strategy changes the power transmission path of the congestion area and achieves reasonable power allocation in low-voltage distribution networks. However, this strategy does not essentially reduce or transfer the total active power during peak hours. Due to the limitations of line capacity, with higher penetration EVs asymmetric access to the networks, the congestion problem of the entire system cannot be totally solved.

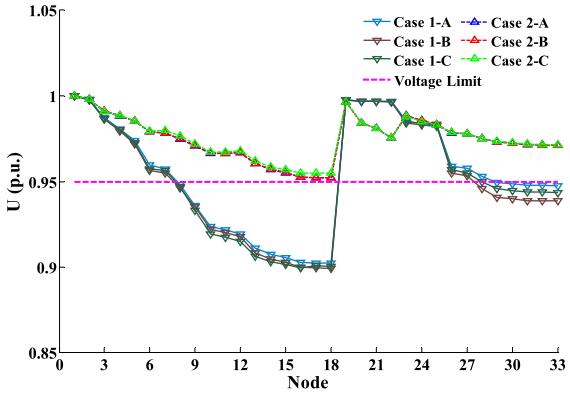

FIGURE 7. Three-phase voltage profile in Case1 and Case 2.

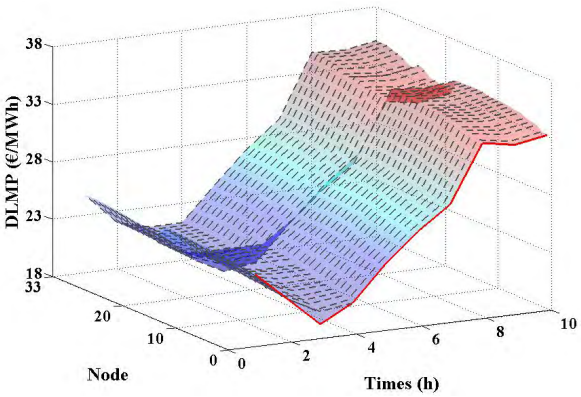

FIGURE 8. DLMP pricing results in phase C.

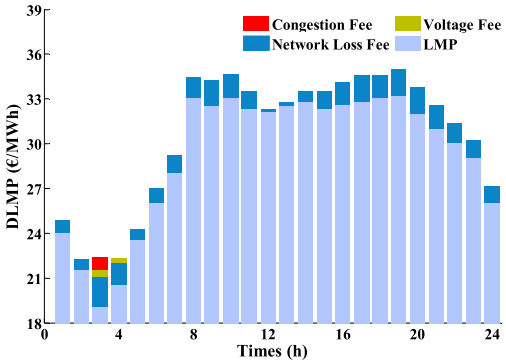

FIGURE 9. DLMP pricing results of node 16 in phase B.

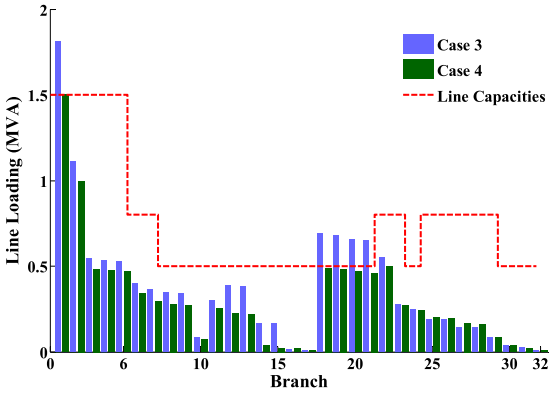

FIGURE 10. Load level of distribution line in Case3 and Case 4.

3) RESULTS AND ANALYSIS OF DLMP PRICING

According to the system parameters and the requirements of flexible load aggregators, DSO formulates the DLMP and issues them to each EV aggregator. Aggregators respond to the DLMP and modify their power consumption plan, which helps eliminate distribution network congestion and voltage violation. The DLMP results for the active power of all the nodes in phase C are obtained as shown in Fig. 8. The red line represents the DLMP in the source node, which is not affected by congestion and voltage deviation. The DLMP in the source node is equal to the base price and the lowest point appears at 3:00 am. To avoid the congestion and voltage violation when the EV's charging demands are high, the electricity pricing during the peak hours is elevated, which motivates the aggregators to disperse the EV's charging demands to a lighter loading period.

In the modified IEEE 33-node distribution system, node 18 is located at the end of a long feeder with the worst operating environment, while node 19 is located near the source node of the system. Thus, the DLMP in node 18 is higher than that in node 19.

Phase B of node 16 is chosen to illustrate the rationality of DLMP pricing. The price is composed of four parts, as shown in Fig. 9. The congestion fee mainly occurs at period 3. During this period, the EV's charging time must be reasonably allocated due to the line capacity limitation.

The yellow part represents the voltage fee. As shown in Fig. 9, a serious voltage drop may occur during the peak charging period, thus introducing the voltage fee. Due to the existence of long feeders in the modified IEEE 33-node distribution system, the system operates in a serious voltage violation condition. The voltage limits are binding at the optimal solution during periods 3 and 4.

The dark blue part represents the fee of network loss calculated based on the reference operating point. Large-scale EVs access to the network brings a higher network loss fee in periods 3 and 4. There is tremendous conventional load power demand from period 16 to 19, and the network loss fees are also at a relatively high level in the meantime.

4) EFFECT OF DLMP ON CONGESTION MANAGEMENT

As shown in Fig. 10, through the proposed congestion management method, the congestion due to EV charging is alleviated.

Fig. 11 shows the three-phase voltage profile in Case 3 and Case 4 during the peak hour. In response to the price signals, the EV charging is expected to take place at the hours with the lowest electricity prices in a wider available period. The three-phase nodal voltage can be well maintained within the

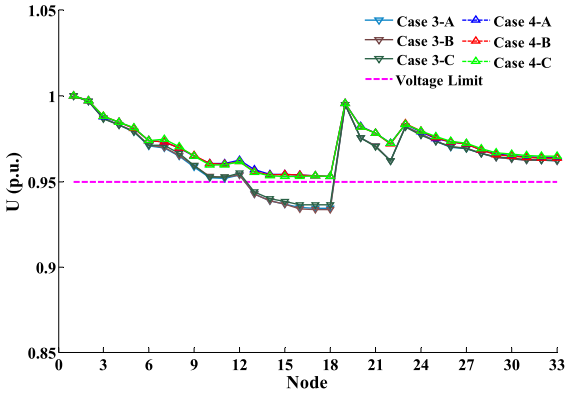

FIGURE 11. Three-phase voltage profile in Case3 and Case 4.

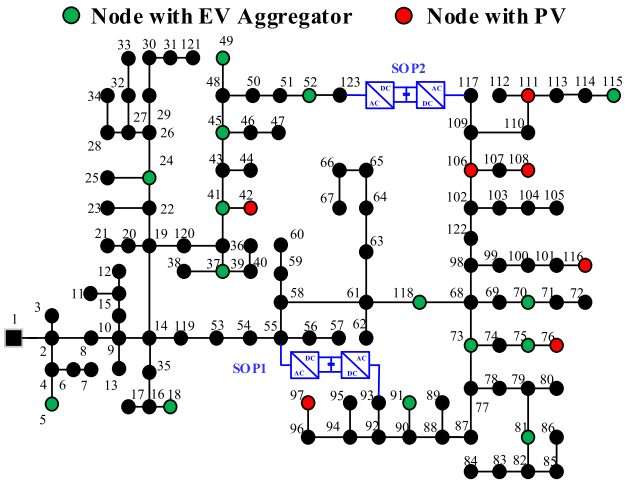

FIGURE 12. Structure of the modified IEEE 123-node system.

voltage limits based the proposed congestion management method.

B. THE MODIFIED IEEE 123-NODE SYSTEM

1) SYSTEM PARAMETER SETTING

The modified IEEE 123-node radial distribution system including a source node and 122 branches is shown in Fig. 3, of which the rated voltage level is 4.16 kV. The total active and reactive load of the system are 3490 kW and 1920 kvar.

The three-phase unbalanced condition seriously exists in this system. There are lots of branches with nonsymmetrical parameters, and maximum load difference among three phases is up to tens of kilowatts. The detailed parameters are provided in [31].

The red nodes are the locations that integrated with PVs. Seven asymmetric access PVs are integrated and operate with a constant power factor of 0.95. The green nodes are the locations that integrated with EV aggregators. Fifteen EV aggregators are integrated into the networks in single-phase charging mode. The simulation result of the EV aggregators with fifty EVs is shown in Fig. 13.

The basic installation parameters are shown in TABLE 4 and TABLE 5.

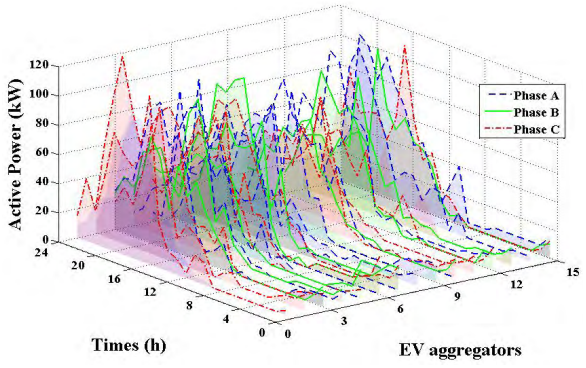

FIGURE 13. Charging plans of EV aggregator with fifty EVs in Case 7 and Case 8.

TABLE 4. Basic installation parameters of DGs.

Parameter	Photovoltaic cells						
Location	42	76	97	106	108	111	116
Phase	C	C	B	C	B	A	C
Capacity (kVA)	200	300	300	150	150	150	200

TABLE 5. Basic installation parameters of EV aggregators.

Parameter	EV aggregators				
Location	5	18	24	37	41
Phase	C	C	ABC	AB	ABC
Location	45	49	52	70	73
Phase	ABC	ABC	ABC	A	ABC
Location	75	81	91	115	118
Phase	C	ABC	B	A	ABC

TABLE 6. Configuration of line capacity limitation.

Branch power flow limitation (kVA)	Branch power flow in normal operation (kVA)
500	<300
800	300–500
1200	500-800
2000	>800

To replace the tie switch in the distribution network, two groups of SOPs with a capability of 500 kVA are installed between nodes 55 and node 93, as well as the nodes 117 and 123, of which the parameters are same with those in subsection V-A.

The line capacities of the branches are listed in Table 6.

2) RESULTS AND ANALYSIS OF SOP BASED CONGESTION MANAGEMENT

Two scenarios are selected for the case studies to verify the effectiveness of SOPs in congestion management. Fifteen EV aggregators are integrated into the networks in

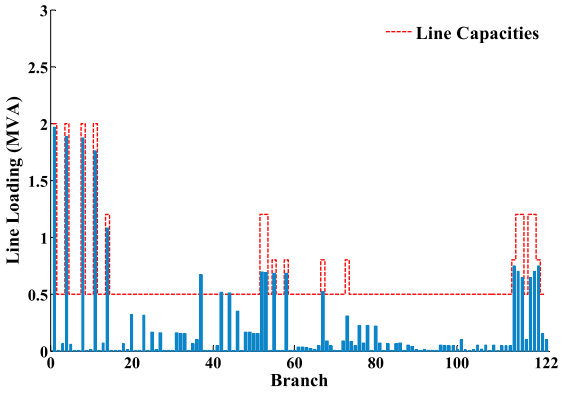

FIGURE 14. Load level of distribution line in Case 5.

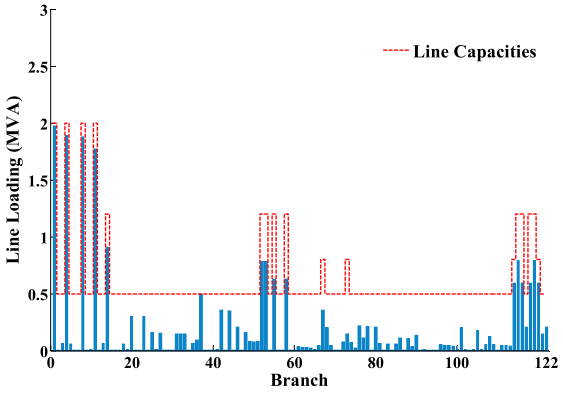

FIGURE 15. Load level of distribution line in Case 6.

single-phase charging mode, and each phase is integrated with twenty-five EVs.

Case 5: This is the base case without any congestion management, and EVs are to charge at the period with the lowest electricity purchase price.

Case 6: DSO uses SOPs to solve the congestion problem, EVs are to charge at the period with the lowest electricity purchase price.

In Fig. 14, the Blue bar represents the heaviest phase loading of the three-phase line. The congestion happens on branches 37, 42 and 44 at 3:00 am in Case 5. In Case 6, with the access of SOPs between nodes 117 and 123, SOPs help supply the load on nodes 41-52, thus eliminating the congestion problem in the low-voltage distribution network. The effects of SOPs on voltage support and reduce network loss have been studied in [32] and are not discussed here.

3) EFFECT OF DLMP ON CONGESTION MANAGEMENT

Two scenarios are selected for the case studies to verify the effectiveness of DLMP in congestion management with high penetration EVs. Fifteen EV aggregators are integrated into the networks in single phase charging mode and each phase is integrated with fifty EVs.

Case 7: DSO uses SOPs to solve the congestion problem, EVs are to charge at the period with the lowest reference purchase price.

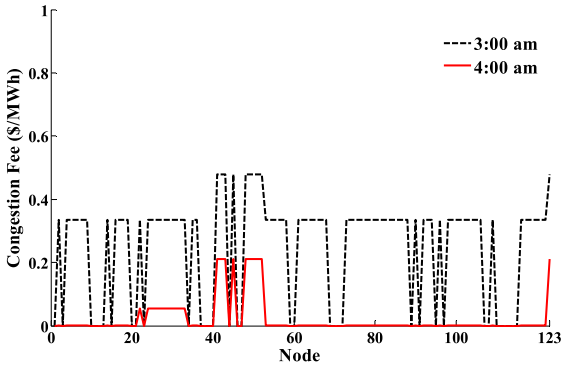

FIGURE 16. Congestion fee at peak charging time in phase C.

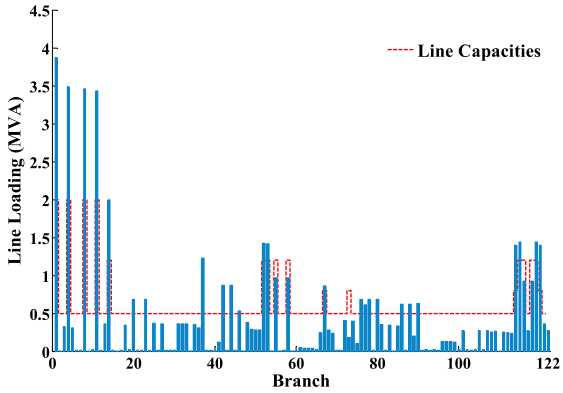

FIGURE 17. Load level of distribution line in Case 7.

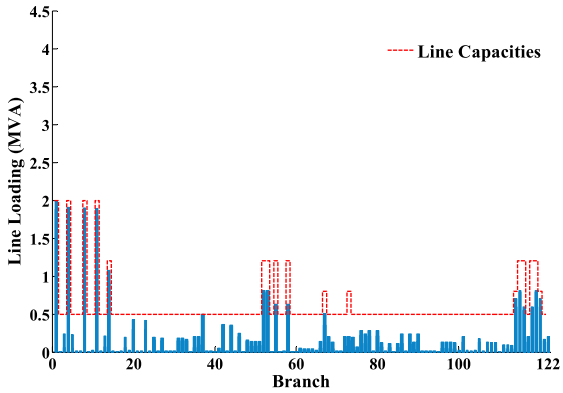

FIGURE 18. Load level of distribution line in Case 8.

Case 8: DSO uses both SOPs and DLMP to solve the congestion problem, DLMPs are delivered to the EV aggregators, which incentivize the EVs to contribute to system operation based on the price signals.

As shown in Fig. 16, a lower basic electricity price would cause line congestion and result in a higher congestion fee. All aggregators tend to charge in lowest price, thus making the congestion situation more serious at 3:00 am. Higher congestion fees are introduced to prevent the line overload caused by the centralized charging.

Fig. 17 and Fig. 18 denote the load level of distribution line in Case 7 and Case 8, the red dotted line represents

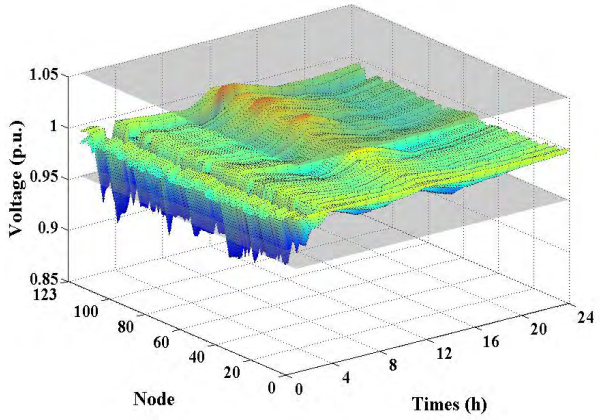

FIGURE 19. Nodal voltage in Case 7.

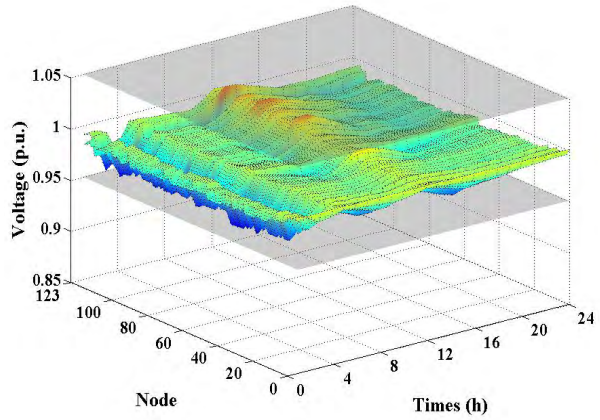

FIGURE 20. Nodal voltage in Case 8.

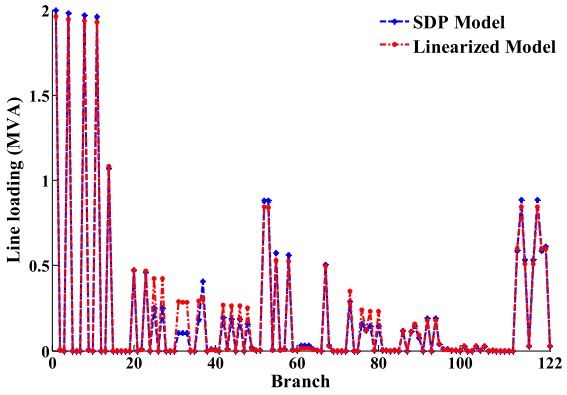

FIGURE 21. The phase C branch power flow in two model.

TABLE 7. Optimization Results of Case 4 and Case 8.

Case	Model	Objective function (€)	Total scheduling cost (€)	Time (s)
4	SDP model	1462.076	23.818	7.14
	Linearized model	1466.640	23.818	0.56
	Actual Power Flow after linearization	1462.115	-	-
8	SDP model	1627.618	50.433	26.88
	Linearized model	1630.338	50.433	1.23
	Actual Power Flow after linearization	1628.747	-	-

the line capacities of the branches. Through the congestion management method proposed in this paper, the congestion due to EV's charging is alleviated.

We noted that branches 1 and 37 approach the limit boundary at the same time. The downstream nodes of branch 37 must consider the congestion fee caused by branches 1 and 37 simultaneously. Thus, the nodes in the downstream of branch 37 have the highest congestion fee (phase C is missing at partial nodes).

The nodal voltages in the two cases are shown in Figs. 19 and 20. The red net surface represents the maximum value of the phase voltage of the node, and the blue net surface represents the minimum value of the phase voltage of the node. A fairly flat and tight voltage profile is attained by the proposed congestion management method.

C. ANALYSIS OF OPTIMIZED RESULT ACCURACY

The EV's charging strategy in the linearized model may be inconsistent with the EVs output strategy in the SDP model, resulting in a slight difference between the actual branch flow and the initial operating point of the system.

In Case 8, the phase C branch power flow in the two models is shown in Fig. 21. Due to the line capacity limitation, the branch currents near the source node are highly consistent. Due to the slight difference between branch line impedance, active power loss of each node is mainly caused by the relatively large power flow branch near the source node. Thus, the network loss approximation can guarantee a certain accuracy during the peak charging period.

The "ratio" quantifies how close an SDP solution to rank one. The solution of proposed model in Case 4 and Case 8 satisfies ratio $\leq 3.75 \times 10^{-8}$ for all matrices in (10). Hence, it is numerically exact. TABLE 7 shows that compared with the SDP model, the linearized model can be solved efficiently with acceptable accuracy.

VI. CONCLUSION

This paper presents a congestion management method for addressing the network loss, voltage violation and line overload problem in low-voltage ADNs. With the ability to realize feeder power flow control of SOPs, DSO enables efficient congestion management of low-voltage distribution networks. Through the SDP conversion, the original NLP model is converted to a symmetrical SDP model via convex relaxation, which can be efficiently solved to meet the demands of rapid centralized control. A DLMP pricing model for unbalanced low-voltage ADNs based on linear approximation is then presented to realize price incentives

for flexible load. Numerical tests empirically show that the proposed method can provide rational DLMP for congestion management in distribution networks with high penetration of EVs.

REFERENCES

[1] A. C. Rueda-Medina and A. Padilha-Feltrin, "Distributed generators as providers of reactive power support—A market approach," *IEEE Trans. Power Syst.*, vol. 28, no. 1, pp. 490–502, Feb. 2013.
[2] J. C. Mukherjee and A. Gupta, "A review of charge scheduling of electric vehicles in smart grid," *IEEE Syst. J.*, vol. 9, no. 4, pp. 1541–1553, Dec. 2015.
[3] N. Leemput, F. Geth, J. Van Roy, A. Delnooz, J. Buscher, and J. Driesen, "Impact of electric vehicle on-board single-phase charging strategies on a Flemish residential grid," *IEEE Trans. Smart Grid*, vol. 5, no. 4, pp. 1815–1822, Jul. 2014.
[4] S. Huang, Q. Wu, Z. Liu, and A. H. Nielsen, "Review of congestion management methods for distribution networks with high penetration of distributed energy resources," in *Proc. IEEE PES Innov. Smart Grid Technol.*, Istanbul, Turkey, Oct. 2014, pp. 1–6.
[5] C. Wang, G. Song, P. Li, H. Ji, J. Zhao, and J. Wu, "Optimal siting and sizing of soft open points in active electrical distribution networks," *Appl. Energy*, vol. 189, pp. 301–309, Mar. 2017.
[6] P. Li *et al.*, "A coordinated control method of voltage and reactive power for active distribution networks based on soft open point," *IEEE Trans. Sustain. Energy*, vol. 8, no. 4, pp. 1430–1442, Oct. 2017.
[7] W. Cao, J. Wu, N. Jenkins, C. Wang, and T. Green, "Benefits analysis of Soft Open Points for electrical distribution network operation," *Appl. Energy*, vol. 165, pp. 36–47, Mar. 2016.
[8] H. Ji, C. Wang, P. Li, F. Ding, and J. Wu, "Robust operation of soft open points in active distribution networks with high penetration of photovoltaic integration," *IEEE Trans. Sustain. Energy*, vol. 10, no. 1, pp. 280–289, Jan. 2019.
[9] R. Li, Q. Wu, and S. S. Oren, "Distribution locational marginal pricing for optimal electric vehicle charging management," *IEEE Trans. Power Syst.*, vol. 29, no. 1, pp. 201–203, Jan. 2014.
[10] S. Huang, Q. Wu, S. S. Oren, R. Li, and Z. Liu, "Distribution locational marginal pricing through quadratic programming for congestion management in distribution networks," *IEEE Trans. Power Syst.*, vol. 30, no. 4, pp. 2170–2178, Jul. 2015.
[11] H. Yuan, F. Li, Y. Wei, and J. Zhu, "Novel linearized power flow and linearized OPF models for active distribution networks with application in distribution LMP," *IEEE Trans. Smart Grid*, vol. 9, no. 1, pp. 438–448, Jan. 2018.
[12] W. Wang and N. Yu, "LMP decomposition with three-phase DCOPF for distribution system," in *Proc. Innov. Smart Grid Technol.-Asia*, Nov./Dec. 2016, pp. 1–8.
[13] L. Bai, J. Wang, C. Wang, C. Chen, and F. Li, "Distribution locational marginal pricing (DLMP) for congestion management and voltage support," *IEEE Trans. Power Syst.*, vol. 33, no. 4, pp. 4061–4073, Jul. 2017.
[14] A. Papavasiliou, "Analysis of distribution locational marginal prices," *IEEE Trans. Smart Grid*, vol. 9, no. 5, pp. 4872–4882, Sep. 2017.
[15] J. Lavaei and S. H. Low, "Zero duality gap in optimal power flow problem," *IEEE Trans. Power Syst.*, vol. 27, no. 1, pp. 92–107, Feb. 2012.
[16] X. Bai, H. Wei, K. Fujisawa, and Y. Wang, "Semidefinite programming for optimal power flow problems," *Elect. Power Energy Syst.*, vol. 30, no. 6, pp. 383–392, Dec. 2008.
[17] S. H. Low, "Convex relaxation of optimal power flow—Part I: Formulations and equivalence," *IEEE Trans. Control Netw. Syst.*, vol. 1, no. 1, pp. 15–27, Mar. 2014.
[18] L. Gan and S. H. Low, "Convex relaxations and linear approximation for optimal power flow in multiphase radial networks," in *Proc. 18th IEEE Power Syst. Comput. Conf. (PSCC)*, Wroclaw, Poland, Aug. 2014, pp. 1–9.
[19] Z. Wang, D. Kirschen, and B. Zhang. (2017). "Accurate semidefinite programming models for optimal power flow in distribution systems." [Online]. Available: https://arxiv.org/abs/1711.07853
[20] B. A. Robbins and A. D. Domínguez-García, "Optimal reactive power dispatch for voltage regulation in unbalanced distribution systems," *IEEE Trans. Power Syst.*, vol. 31, no. 4, pp. 2903–2913, Jul. 2016.
[21] X. Chen, W. Wu, and B. Zhang, "Robust capacity assessment of distributed generation in unbalanced distribution networks incorporating ANM technique," *IEEE Trans. Sustain. Energy*, vol. 9, no. 2, pp. 651–663, Apr. 2018.
[22] *Voltage Characteristics of Electricity Supplied by Public Electricity Networks*, Cenelec Standard EN 50160, 2010.
[23] F. Li and R. Bo, "DCOPF-based LMP simulation: Algorithm, comparison with ACOPF, and Sensitivity," *IEEE Trans. Power Syst.*, vol. 22, no. 4, pp. 1475–1485, Nov. 2007.
[24] S. Wang, S. Chen, L. Ge, and L. Wu, "Distributed generation hosting capacity evaluation for distribution systems considering the robust optimal operation of OLTC and SVC," *IEEE Trans. Sustain. Energy*, vol. 7, no. 3, pp. 1111–1123, Jul. 2016.
[25] J. Lofberg, "YALMIP: A toolbox for modeling and optimization in MATLAB," in *Proc. CASCD Conf.*, 2004, pp. 284–289.
[26] M. E. Baran and F. F. Wu, "Optimal capacitor placement on radial distribution systems," *IEEE Trans. Power Del.*, vol. 4, no. 1, pp. 725–734, Jan. 1989.
[27] Z. Tian, W. Wu, B. Zhang, and A. Bose, "Mixed-integer second-order cone programing model for VAR optimization and network reconfiguration in active distribution networks," *IET Gener. Transmiss. Distrib.*, vol. 10, no. 8, pp. 1938–1946, May 2016.
[28] S. Xu *et al.*, "Ant-based swarm algorithm for charging coordination of electric vehicles," *Int. J. Distrib. Sensor Netw.*, vol. 9, no. 5, pp. 607–610, May 2013.
[29] H. Su *et al.*, "Three-phase load balancing charging line selection device and simulation analysis of large-scale electric vehicle," *Electr. Power Autom. Equip.*, vol. 38, no. 6, pp. 103–108, Mar. 2018.
[30] K. Chen, W. Wu, B. Zhang, and H. Sun, "Robust restoration decision-making model for distribution networks based on information gap decision theory," *IEEE Trans Smart Grid*, vol. 6, no. 2, pp. 587–597, Mar. 2015.
[31] W. H. Kersting, "Radial distribution test feeders," *IEEE Trans. Power Syst.*, vol. 6, no. 3, pp. 975–985, Aug. 1991.
[32] P. Li *et al.*, "Optimal operation of soft open points in active distribution networks under three-phase unbalanced conditions," *IEEE Trans. Smart Grid*, vol. 10, no. 1, pp. 380–391, Jan. 2019.

JINLI ZHAO (M'11) received the B.S. and Ph.D. degrees in electrical engineering from Tianjin University, Tianjin, China, in 2001 and 2007, respectively, where she is currently an Associate Professor with the School of Electrical and Information Engineering.

Her current research interests include power system security and stability, smart distribution network simulation, and optimal control.

YUSHUO WANG was born in Tianjin, China, in 1994. He received the B.S. degree in electrical engineering from Tianjin University, Tianjin, China, in 2016, where he is currently pursuing the M.Sc. degrees with the School of Electrical and Information Engineering. His current research interest includes congestion management of smart distribution systems.

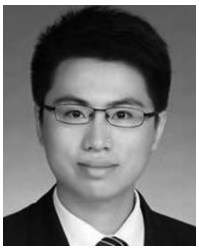

GUANYU SONG (M'17) received the B.S. and Ph.D. degree in electrical engineering from Tianjin University, Tianjin, China, in 2012 and 2017, respectively, where he is currently a Lecturer with the School of Electrical and Information Engineering.

His current research interests include optimal planning and operation of smart distribution systems.

PENG LI (M'11) received the B.S. and Ph.D. degrees in electrical engineering from Tianjin University, Tianjin, China, in 2004 and 2010, respectively, where he is currently an Associate Professor with the School of Electrical and Information Engineering.

His current research interests include distributed generation systems and microgrids, smart distribution systems, active distribution networks, and transient simulation and analysis.

CHENGSHAN WANG (SM'11) received the Ph.D. degree in electrical engineering from Tianjin University, Tianjin, China, in 1991, where he is currently a Professor with the School of Electrical and Information Engineering.

From 1994 to 1996, he was a Senior Academic Visitor with Cornell University, Ithaca, NY, USA. From 2001 to 2002, he was a Visiting Professor with the Carnegie Mellon University, Pittsburgh, PA, USA. He is also the Director of the Key Laboratory of Smart Grid of Ministry of Education, Tianjin University. His current research interests include distribution system analysis and planning, distributed generation systems and microgrids, and power system security analysis.

Dr. Wang is an Editorial Board Member of *Applied Energy* and the *Journal of Modern Power Systems and Clean Energy*.

JIANZHONG WU (M'14) received the Ph.D. degree from Tianjin University, Tianjin, China, in 2004.

From 2004 to 2006, he was with Tianjin University, where he is currently an Associate Professor. From 2006 to 2008, he was a Research Fellow with The University of Manchester, Manchester, U.K. He is currently a Professor with the School of Engineering, Institute of Energy, Cardiff University, London, U.K. His current research interests include energy infrastructure and smart grids.

Dr. Wu is a member of the Institution of Engineering and Technology and the Association for Computing Machinery.